



HAL
open science

Prediction of water retention properties of Syrian clayey soils

Hassan Al Majou, Fabrice Muller, Philippe Penhoud, Ary Bruand

► **To cite this version:**

Hassan Al Majou, Fabrice Muller, Philippe Penhoud, Ary Bruand. Prediction of water retention properties of Syrian clayey soils. Arid Land Research and Management, 2021, 10.1080/15324982.2021.1965674 . hal-03326818

HAL Id: hal-03326818

<https://hal.science/hal-03326818v1>

Submitted on 26 Aug 2021

HAL is a multi-disciplinary open access archive for the deposit and dissemination of scientific research documents, whether they are published or not. The documents may come from teaching and research institutions in France or abroad, or from public or private research centers.

L'archive ouverte pluridisciplinaire **HAL**, est destinée au dépôt et à la diffusion de documents scientifiques de niveau recherche, publiés ou non, émanant des établissements d'enseignement et de recherche français ou étrangers, des laboratoires publics ou privés.

1 Prediction of water retention properties of Syrian clayey soils

2 Hassan Al Majou^{a,b}, Fabrice Muller^{a,c}, Philippe Penhoud^a, Ary Bruand^a

3 ^aUniversité d'Orléans, CNRS, BRGM. Institut des Sciences de la Terre d'Orléans (ISTO), UMR 7327,
4 1A rue de la Férollerie, CS 20066, 45071 Orléans Cedex 2, France ; ^bUniversity of Damas,
5 Department of Soil Science, Faculty of Agronomy, PO Box 30621, Syria ; ^cUniversité d'Orléans,
6 CNRS, Interfaces, Confinement, Matériaux et Nanostructures (ICMN), UMR 7374, 1B, rue de la
7 Férollerie, CS 40059, 45071 Orléans Cedex 2, France.

8

9 Corresponding author: Ary.Bruand@univ-orleans.fr, Tel: 33(0)238492534, Fax: 33(0)238494476,
10 Université d'Orléans, CNRS, BRGM. Institut des Sciences de la Terre d'Orléans (ISTO), 1A rue de la
11 Férollerie, CS 20066, 45071 Orléans Cedex 2, France

12

13

14

15 **ABSTRACT**

16 Studies on clayey soils developed in temperate areas have shown that their water retention properties
17 are related to both the clay content and the specific pore volume of the clay, the latter being related to
18 the hydric history of the soil. Our objective was to discuss the validity of these results for clayey soils
19 developed in semi-arid areas. Samples were collected in soils located in Syria. Physico-chemical
20 properties were determined. Water content was measured at field capacity and for water potentials
21 ranging from -10 to -15000 hPa. X-ray diffraction analyses were performed on the clay fraction to
22 identify the clay. Results showed that the clays have both a high cation exchange capacity (0.707 to
23 0.891 mmol+ per g of clay) and a high external specific surface area (112 and 178 m² per g of clay).

24 These values are consistent with the X-ray diffraction results which showed the presence of a high
25 proportion of smectite in most horizons and secondarily of varying proportions of illite and chlorite;
26 kaolinite, while present, was not abundant. Results also showed that the amount of water retained by
27 the clay according to the water potential was closely related to the specific pore volume of the clay at
28 field capacity. Regression equations established by using both the data published earlier and those of
29 this study enabled us to predict the water retention properties of clayey soils for a larger range of clay
30 mineralogy and climatic environments including semi-arid environments than previously discussed in
31 the literature.

32

33 **Keywords:** Clay content, Bulk density, Cation exchange capacity, Specific surface area, X-ray
34 diffraction, Pedotransfer function.

35

36 **Introduction**

37 Clayey soils are often intensively cultivated in semi-arid and arid areas, particularly when irrigation is
38 available (e.g., Ethan & Umar 2001; Mason et al., 2015). Their physical properties are closely related
39 to the clay content and clay characteristics such as their mineralogical nature, the size of the
40 elementary clay particles and the nature of the exchangeable cations (Tessier & Pédro 1987; Quirk
41 1994; Wilson 1999; Churchman & Velde 2019). Whatever the soil texture and more markedly in semi-
42 arid and arid areas, it is important to ascertain the water retention properties of soils in order to manage
43 the water supply and consequently crop growth appropriately (Gaiser et al., 2000). To accomplish this,
44 pedotransfer functions that enable prediction of the water retention properties of soils have therefore
45 been developed (e.g., Bouma & Van Lanen 1987; Wösten et al., 1999; Al Majou et al., 2008a &
46 2008b; Ostovari et al., 2015; Kalumba et al., 2020; Singh et al., 2020; Xu Xu et al., 2021), with several
47 studies focusing on soils of semi-arid and arid areas (Tóth et al., 2012; Khlosi et al., 2012 & 2016; Al
48 Majou et al., 2018; De Paepe et al., 2018; Santra et al., 2018; Dharumarajan et al., 2019; Soleimani et

49 al., 2020). At the same time, some studies aimed at a better understanding of the water retention
50 properties of soils according to the characteristics of their clay minerals but the validity of the results
51 for soils of semi-arid and arid areas remains unclear (Gaiser et al., 2000; Moret-Fernandez et al.,
52 2013). For clayey soils developed on sedimentary materials, Bruand and Tessier (2000) showed that
53 relationships between water retention properties and clay particles characteristics can be established.
54 The clay particles, thanks to their fine size ($< 2\mu\text{m}$), play a privileged role in water retention and soil
55 structuring but also in the retention and bioavailability of chemical elements essential for plants
56 (Bergaya & Lagaly 2013; Churchman & Velde 2019). Depending on the characteristics of clay
57 particles, i.e. both their size and shape, the nature of the cations in the interlayer space and on the
58 external surfaces, the clay fabric, which corresponds to both the volume of clay particles and the
59 associated pore volume resulting from their assemblage, can vary highly from one soil to another, with
60 significant consequences for the water retention properties of the soil (Tessier et al., 1992; Bruand &
61 Tessier, 2000; Boivin et al., 2004). However, most studies on the water retention properties of clayey
62 soils were developed for clayey soils in temperate areas and their validity for clayey soils in other
63 climate areas is still under discussion. D'Angelo et al. (2014) studied the high sensitivity to drought of
64 Chinese red clay soils developed on clayey sediments in humid subtropical areas. They showed that it
65 was related to a very dense clay fabric which resulted from a high degree of consolidation, leading to a
66 small porosity able to retain water available for plants. Other clayey soils in tropical and subtropical
67 areas exhibit a strong micro-granular structure and their water retention properties are closely related
68 to both inter- and intra-microgranular porosity (Balbino et al., 2004; Tawornpruek et al., 2005; Reatto
69 et al., 2007). In this study, the objective was to analyze the water retention properties of clayey soils
70 developed in semi-arid areas of Syria and to show how results recorded in earlier work on soils located
71 in temperate areas (Bruand & Zimmer, 1992; Bruand & Tessier, 2000; Al Majou et al., 2008a) can be
72 applied to the soils studied. We discuss how both the clay content and pore volume developed by the
73 clay fabric, the latter being related to clay mineralogy and size of the elementary clay particles as well
74 as the hydric history, can be used to predict the water retention properties of the clayey soils studied.

75

76 **Materials and methods**

77 *The soils studied*

78 The soils studied are located in semi-arid areas of Syria (Rigot 2006) between latitudes 32 and 41° N
79 and longitudes 35 to 42° E. A set of 10 samples (clay content > 0.3 g g⁻¹) including 4 horizons A and 6
80 horizons B were collected in 5 clayey soils located in the vicinity of the towns of Jabah (JB 1 and
81 JB 2), Al-Suwayda (SW 1), Al-Tha'Ala (TH 1) and Al-Qamishli (QM 1) (Table 1). The soils
82 developed on clayey surface formations including coarse elements of basic extrusive rocks or
83 calcareous alluvium parent materials (Table 1). They are Cambisols (JB 1 and JB 2), Vertisols (SW 1
84 and TH 1) and a Clacisol (QM 1) according to the IUSS Working Group WRB (2015) (Tableau 1) and
85 all Inceptisols according to the USDA Soil taxonomy (Soil Survey Staff, 2010) (Table 1). They are
86 representative of the major Syrian clayey soils (Land Classification and Soil Survey of the Syrian
87 Arab Republic, 1982) in two Syrian agro-climatic areas as defined by Khlosi et al. (2012).

88

89 *Physico-chemical and hydric analyses*

90 Undisturbed roughly parallelepiped samples 500-800 cm³ in volume were collected in winter when the
91 soil was near to field capacity and as a consequence near maximum swelling. The samples were stored
92 at 4-5°C to reduce biological activity and in sealed plastic containers to avoid water loss.

93 Part of the samples was air-dried and manually ground in a mortar to < 2 mm material. Particle-
94 size distribution was measured using the pipette method after pretreatment with hydrogen peroxide
95 and sodium hexametaphosphate (Robert & Tessier 1974). The CaCO₃ content (*CaCO₃*, in g per g of
96 oven-dried soil) was measured according to Dupuis (1969). Cation exchange capacity (*CEC*, in mmol₊
97 per g of oven-dried soil) and exchangeable cations (in mmol₊ per g of oven-dried soil) were measured
98 using ammonium acetate buffered at pH 7.0, and organic carbon content (*OC*, in g per g of oven-dried
99 soil) by oxidation using an excess amount of potassium bichromate in sulphuric acid controlled at

100 135°C (Baize, 2018). The N₂-BET external specific surface area (*SSA*, in m² per g of oven-dried soil)
101 was measured for the < 2 mm fraction dried at 105 °C (Fripiat et al., 1971).

102 Centimetric clods (5 to 10 cm³) were separated by hand from the stored decametric samples.
103 Their water content at field capacity (*W_{fc}*, in g of water per g of oven dried soil) and bulk density (*D_b*)
104 were measured using the kerosene method (Monnier et al., 1973). The gravimetric water content (*W*,
105 in g of water per g of oven-dried soil) at water potentials, *h*, of -10, -33, -100, -330, -1000, -3300
106 and -15000 hPa was measured using a pressure membrane or pressure plate apparatus. The clods were
107 placed on a paste made of < 2 μm particles of kaolinite to establish continuity of water between the
108 clods and the membrane or the porous plate of the apparatus (Bruand et al., 1996).

109 The mineralogical composition of the < 2 μm material of the horizons was determined by X-ray
110 diffraction (XRD) using the air dried < 2 mm material. The clay fraction was collected using the
111 sedimentation method at 20°C after mechanical dispersion and saturated with Mg⁺⁺ according to
112 Robert and Tessier (1974). Oriented clay deposits were prepared on glass slides and studied using an
113 X-ray diffractometer equipped with a Si(Li) solid detector to filter the Cu_{kα} radiation ($\lambda_{Cu_{k\alpha}} =$
114 1.5418 Å) of a standard European type X-ray tube (40 kV, 40 mA). The XRD patterns were collected
115 from 2 to 24° 2θ per step of 0.05° 2θ, on successively air-dried at 20°C, glycoled, heated to 150 and
116 then 550°C oriented clay deposits (Robert & Tessier 1974; Bruand & Prost 1986).

117

118 ***Criteria used to evaluate the performance of the regression equations***

119 The performance of the regression equations established to predict the gravimetric water of the
120 horizons was assessed using the mean error (*ME*), the standard deviation (*SD*) and the root mean
121 square error (*RMSE*):

$$122 \quad ME = \frac{1}{l} \sum_{j=1}^l (W_{p,i,j} - W_{m,i,j}) \quad (1)$$

123
$$SD = \left\{ \frac{1}{l} \sum_{j=1}^l [(W_{p,i,j} - W_{m,i,j}) - ME]^2 \right\}^{1/2} \quad (2)$$

124
$$RMSE = \left\{ \frac{1}{l} \sum_{j=1}^l (W_{p,i,j} - W_{m,i,j})^2 \right\}^{1/2} \quad (3)$$

125 where $W_{p,i,j}$ is the predicted gravimetric water content of the horizon at matric potential i for the
 126 horizon j , $W_{m,i,j}$ is the measured gravimetric water content of the horizon at matric potential i for the
 127 horizon j , and l is the number of horizons studied.

128 In the same way, ME , SD and $RMSE$ were calculated to evaluate the performance of the equations
 129 used to predict the volumetric water content of the horizons as follows:

130
$$ME = \frac{1}{l} \sum_{j=1}^l (\theta_{p,i,j} - \theta_{m,i,j}) \quad (4)$$

131
$$SD = \left\{ \frac{1}{l} \sum_{j=1}^l [(\theta_{p,i,j} - \theta_{m,i,j}) - ME]^2 \right\}^{1/2} \quad (5)$$

132
$$RMSE = \left\{ \frac{1}{l} \sum_{j=1}^l (\theta_{p,i,j} - \theta_{m,i,j})^2 \right\}^{1/2} \quad (6)$$

133 where $\theta_{p,i,j}$ is the predicted volumetric water content of the horizon at matric potential i for the horizon
 134 j , $\theta_{m,i,j}$ is the measured volumetric water content of the horizon at matric potential i for the horizon j ,
 135 and l is the number of horizons studied.

136 The values of ME and SD provide information on the estimation bias and precision, respectively.
 137 The sign of ME indicates whether the prediction overestimated (positive) or underestimated (negative)
 138 the value predicted. As for $RMSE$, it varies according to both the overall prediction bias and overall
 139 prediction precision. The calculation of ME gives equal weight to all errors whereas $RMSE$ assigns
 140 more weight to larger errors than to smaller ones. The greater the difference between ME and $RMSE$,
 141 the more large errors there are. Thus, the best prediction performance is recorded when ME is as close
 142 as possible to 0 and SD and $RMSE$ are as small as possible, indicating the most unbiased and precise
 143 prediction.

144

145 **Results**

146 *Physico-chemical characteristics*

147 The main characteristics of the studied samples are given in Table 2. The horizons studied showed
148 very low or low CaCO_3 content ($\leq 0.06 \text{ g g}^{-1}$) except for the horizons QML 1-1 and 1-2 for which the
149 CaCO_3 content was 0.30 and 0.31 g g^{-1} , respectively. The organic carbon content ranged from 0.002 to
150 0.008 g g^{-1} , the highest organic carbon content being recorded for the horizons A. The clay content
151 (CC , in g per g of oven-dried soil at 105°C) ranged from 0.43 to 0.69 g g^{-1} between the different
152 horizons studied but did not vary highly with depth in each soil (Table 2). The cation exchange
153 capacity (CEC , in mmol_+ per g of oven-dried soil at 105°C) ranged from 0.304 to $0.492 \text{ mmol}_+ \text{ g}^{-1}$.
154 The external specific surface area (SSA , in m^2 per g of oven-dried soil at 105°C) ranged from 61 to
155 $91 \text{ m}^2 \text{ g}^{-1}$.

156

157 *Clay mineralogy*

158 The XRD patterns of the clay extracted from the horizons studied showed (Figure 1) the presence of
159 different types of clays (Robert & Tessier 1974; Bruand & Prost 1986; Moore & Reynold 1997):

- 160 – 1:1 clays which are kaolinite as shown by the peak at 0.72 nm which is similar at 20°C , 150°C
161 and after treatment with ethylene glycol. The absence of a peak at 0.72 nm after heating to
162 550°C confirmed the presence of kaolinite which is dehydroxylated at such a temperature;
- 163 – non-swelling 2:1 clays which are illite as shown by the peak at $1.12\text{--}1.02 \text{ nm}$ at 20°C which
164 did not change after treatment with ethylene glycol. After heating at 550°C , this peak shifted
165 to 1.01 nm , indicating the closing of the magnesian interlamellar spaces;

- 166 – swelling 2:1 clays which are smectite as shown by the shift of the wide peak at 1.44–1.57 nm
167 at 20°C to 1.72–1.77 nm after treatment with ethylene glycol because of the swelling of the
168 interlamellar space due to intercalation of the ethylene glycol molecules. After heating at
169 550°C, all the peaks recorded for higher values than 1.01 nm disappeared, indicating the
170 closing of the magnesian interlamellar spaces due to the loss of the ethylene glycol molecules;
- 171 – 2:1/1 clays which are chlorites as shown by the peak at 1.42–1.47 nm similar at 20°C and after
172 treatment with ethylene glycol. The remaining peak at 1.42 nm recorded after heating at
173 550°C is indeed consistent with the presence of chlorites which are not dehydroxylated at such
174 a temperature.

175 A semi-quantitative evaluation of the content in the different types of clays identified is given in Table
176 3.

177

178 *Water retention properties*

179 The water retention properties showed a wide variety of water content between –10 and –15000 hPa
180 matric water potential (Table 4). The smallest and highest water contents at field capacity were 0.262
181 and 0.507 g g⁻¹, respectively. This high variation in water content at field capacity was consistent with
182 the water content recorded at –10 hPa which ranged from 0.328 to 0.540 g g⁻¹ and at –15000 hPa
183 which ranged from 0.207 to 0.385 g g⁻¹.

184

185 **Discussion**

186 *Physico-chemical characteristics and clay mineralogy*

187 As the soil horizons contained little organic carbon (Table 2), which is consistent with the soil organic
188 matter dynamics in semi-arid areas (Mrabet, 2011; Schellekens et al., 2013), the contribution of

189 organic matter to the cation exchange capacity was considered as being negligible compared with the
190 cation exchange capacity of the clay. Indeed, if we assume that the cation exchange capacity of the
191 organic matter of the soil studied is equal to $4 \text{ mmol}_+ \text{ g}^{-1}$ of organic carbon, which is a value among
192 the highest values recorded in the literature (Schnitzer, 1978; Tate & Theng, 1980; Stevenson, 1982),
193 the contribution of organic matter to the *CEC* would range from 0.008 to $0.032 \text{ mmol}_+ \text{ g}^{-1}$ of oven
194 dried soil for the horizons studied. Thus, the cation exchange capacity of the clay (CEC_{cl} , in mmol_+ per
195 g of oven-dried clay at 105°C) was calculated as follows:

$$196 \quad CEC_{cl} = (CEC/CC) \quad (7)$$

197 with *CC* the clay content. Results showed that CEC_{cl} ranged from 0.707 to $0.891 \text{ mmol}_+ \text{ g}^{-1}$ (Table 5),
198 indicating that the clay fraction was mainly composed of swelling 2:1 clays (Robert & Tessier 1974;
199 Wilson, 1999; Churchman & Velde 2019). These values of CEC_{cl} are consistent with the X-ray
200 diffraction data (Figure 1) which show the predominance of 2/1 clay minerals with smectite content
201 ranging from not abundant to abundant depending on the horizon (Table 3).

202 As the calculated surface area developed by quartz spheres with a diameter $> 2 \mu\text{m}$ was $< 1.1 \text{ m}^2$
203 g^{-1} , the contribution of both the silt and sand particles can be assumed to range from 0.2 to $0.6 \text{ m}^2 \text{ g}^{-1}$
204 for the soil studied and therefore negligible compared to the *SSA* measured (Table 2). Thus, the
205 external specific surface area (*SSA*) of the clay fraction was calculated (SSA_{cl} , m^2 per g of oven-dried
206 clay at 105°C) as follows:

$$207 \quad SSA_{cl} = (SSA/CC) \quad (8)$$

208 The results showed that SSA_{cl} ranged from 112 to $178 \text{ m}^2 \text{ g}^{-1}$ (Table 5) which are high external specific
209 surface areas for clays, indicating a very small size of the elementary clay particles in the horizons
210 studied (Bergaya & Lagaly 2013; Churchman & Velde 2019).

211 Compared to the 37 clayey soils studied by Bruand and Tessier (2000), the CEC_{cl} recorded for the
212 Syrian clayey soils studied were higher. The SSA_{cl} recorded in this study were also higher than those
213 recorded by Bruand and Tessier (2000) except for the horizons JB 1 and JB 2 for which the SSA_{cl} were

214 among the highest recorded by these authors. To extend the range of both the CEC_{cl} and SSA_{cl}
215 discussed, the relationship between CEC_{cl} and SSA_{cl} was established using both the data published by
216 Bruand and Tessier (2000) and those recorded in this study (Figure 2). The closeness of the
217 relationship ($R^2 = 0.78$, $n = 47$) is consistent with the results recorded by Bruand and Zimmer (1992)
218 and Bigorre et al. (2000), indicating that a high proportion of CEC_{cl} variance was explained by SSA_{cl}
219 for the soils studied and consequently by the size of the elementary clay particles (Figure 2). Thus, the
220 cation exchange capacity of the elementary clay particles appears to be mainly related to the negative
221 charges present on the external surfaces of these particles (Robert et al., 1991; Bergaya & Lagaly
222 2013). The high distance to the regression line recorded for the horizons TH 1-2, TH 1-3, QM 1-1 and
223 QM 1-2 indicates that the interfoliar space of the elementary clay particles, which SSA_{cl} does not
224 account for, contributes more than for the other horizons to their cation exchange capacity (Figure 2,
225 Table 5) (Bergaya & Lagaly 2013; Churchman & Velde 2019).

226 Comparison of the XRD patterns with the values of CEC_{cl} and SSA_{cl} recorded showed the
227 presence of a small amount of smectite for JB 2-1, JB 2-2 and JB 2-3 when CEC_{cl} and SSA_{cl} were
228 among the highest values recorded (Figure 1, Tables 3 and 5). The low intensity of the peak between
229 1.44 and 1.57 nm at 20°C and between 1.72 and 1.77 nm after treatment with ethylene glycol
230 (Figure 1) is in all likelihood related to the weak organization along the crystallographic plane ab of
231 the elementary clay particles in the clay deposit on the glass slide because of the very small size of the
232 elementary clay particles as indicated by SSA_{cl} (Table 5) (Tessier & Pédro 1987). The proportion of
233 smectite in JB 2-1, JB 2-2 and JB 2-3 is therefore probably higher than that indicated by the XRD
234 patterns (Figure 1) and reported in Table 3.

235

236 ***Pore volume developed by the assemblage of elementary clay particles***

237 Assuming that water was mainly retained by the clay phase whatever the potential, as earlier shown by
238 Bruand and Zimmer (1992), Bruand and Tessier (2000) and D'Angelo et al. (2014), we considered
239 that for the centimetric clods at field capacity the volume of cracks and biopores was negligible

240 compared with the pore volume developed by the assemblage of the elementary clay particles. Thus,
241 the specific volume of clods at the field conditions (V_{fc}) is related to the specific volume of the solid
242 phase (V_s , in cm^3 per g of oven-dried soil) and to the specific pore volume (V_p , in cm^3 per g of oven-
243 dried soil) as follows:

$$244 \quad V_{fc} = V_s + V_p \quad (9)$$

245 V_p was calculated for each horizon using $V_s = 0.377 \text{ cm}^3 \text{ g}^{-1}$ which corresponds to a particle density of
246 2.65 and V_{fc} which corresponds to the reciprocal of D_b measured on centimetric clods (Table 2),
247 giving:

$$248 \quad V_p = (1/D_b) - V_s \quad (10)$$

249 The values of V_p recorded ranged from 0.671 to 0.840 $\text{cm}^3 \text{ g}^{-1}$. The specific pore volume of the clay
250 ($V_{p,cl}$, in cm^3 per g of oven-dried clay) was calculated as follows:

$$251 \quad V_{p,cl} = V_p / CC \quad (11)$$

252 The quantity $V_{p,cl}$, which can be considered as a quantitative expression of the clay fabric, ranged from
253 0.612 to 0.722 $\text{cm}^3 \text{ g}^{-1}$ (Table 5). This is a much smaller range of variation than that recorded for the
254 soils studied by Bruand and Tessier (2000) ($0.337 \leq V_{p,cl} \leq 1.484 \text{ cm}^3 \text{ g}^{-1}$). However, it is interesting to
255 note that although the values of CEC_{cl} recorded for the Syrian clayey horizons studied are higher than
256 those recorded for the clayey soils studied by Bruand and Tessier (2000), 6 soils of those studied by
257 the latter showed higher $V_{p,cl}$ than those recorded in this study, thus illustrating that $V_{p,cl}$ varies
258 according to the clay mineralogy but also according to the hydric history of the soil (Tessier and
259 Pédro, 1984 and 1987). In the same way, even if $V_{p,cl}$ could theoretically be assumed to be closely
260 related to the size of the elementary clay particles, the results recorded showed the lack of a close
261 relationship between $V_{p,cl}$ and SSA_{cl} , again because of the hydric history of the soil (Tessier and Pédro,
262 1984 and 1987). This is the case of the Syrian clayey soils studied with a very poor relationship
263 between $V_{p,cl}$ and SSA_{cl} ($R^2 = 0.24$).

264

265 ***Water retention properties of the clay***

266 Since the difference in water retention properties between the horizons results from the variation in
267 both the clay content and the water retention properties of the clay, the latter were calculated by
268 correcting the gravimetric water content of the horizon (W) for clay content (CC) at different water
269 potentials as follows:

270
$$W_{cl} = W/CC \quad (12)$$

271 The quantity W_{cl} can be considered as the amount of water retained by the pore volume related to the
272 clay fabric (W_{cl} , in g of water per g of oven-dried clay). Regression equations were established
273 between W_{cl} and $V_{p,cl}$ with the data published by Bruand and Tessier (2000) and then with both the data
274 published by these authors and those recorded in this study for Syrian clayey soils (Table 6).

275 Although the range of variation of CEC_{cl} and SSA_{cl} was markedly different between, on the one
276 hand, the dataset published by Bruand and Tessier (2000) with CEC_{cl} ranging from 0.227 to 0.666
277 $\text{mmol}_+ \text{g}^{-1}$ and SSA_{cl} ranging from 53 to 139 $\text{m}^2 \text{g}^{-1}$ and, on the other hand, the Syrian dataset with
278 CEC_{cl} ranging from 0.707 to 0.891 $\text{mmol}_+ \text{g}^{-1}$ and SSA_{cl} from 112 to 178 $\text{m}^2 \text{g}^{-1}$ (Table 5), the
279 regression equations established by Bruand and Tessier (2000) (Table 6) were tested with the Syrian
280 dataset to be able to discuss the expected improvement in the prediction quality when the regression
281 equations are established with both datasets (Table 7). Their performance was evaluated using ME , SD
282 and $RMSE$. Results showed that ME ranged from -0.065 g g^{-1} at -10 hPa water potential to 0.047 g g^{-1}
283 at -1000 hPa water potential (mean = -0.008 g g^{-1}), SD from 0.042 g g^{-1} at -15000 hPa water potential
284 to 0.069 g g^{-1} at -330 hPa water potential (mean = 0.057 g g^{-1}) and $RMSE$ from 0.051 g g^{-1} at -3300
285 hPa water potential to 0.091 g g^{-1} at -10 hPa water potential (mean = 0.068 g g^{-1}) (Table 7).

286 Regression equations were established between W_{cl} and $V_{p,cl}$ using both the data recorded by
287 Bruand and Tessier (2000) and the data recorded in this study (Table 6). They were tested successively
288 on the two datasets by recalculating them each time without taking into account the horizon on which

289 they were tested. The number of horizons used to establish the regression equations was 46, one being
290 left out when calculating each regression equation. When tested on the dataset published by Bruand
291 and Tessier (2000), results showed that *ME* ranged from -0.011 g g^{-1} at -330 hPa and -1000 hPa
292 water potential to 0.014 g g^{-1} at -10 hPa water potential (mean = 0.001 g g^{-1}), *SD* from 0.035 g g^{-1} at $-$
293 3300 hPa water potential to 0.043 g g^{-1} at -10 hPa water potential (mean = 0.039 g g^{-1}) and *RMSE*
294 from 0.035 g g^{-1} at -3300 hPa water potential to 0.045 g g^{-1} at -10 hPa water potential according
295 (mean = 0.040 g g^{-1}) (Table 7). When tested on the Syrian clayey soils, results showed a lower
296 prediction performance than when tested on the French dataset, with *ME* ranging from -0.052 g g^{-1} at
297 -10 hPa water potential to 0.037 g g^{-1} at -1000 hPa water potential (mean = -0.006 g g^{-1}), *SD* from
298 0.043 at -15000 hPa water potential to 0.070 g g^{-1} at -330 hPa water potential (mean = 0.058 g g^{-1}) and
299 *RMSE* from 0.050 g g^{-1} at -3300 hPa water potential to 0.083 g g^{-1} at -10 hPa water potential (mean =
300 0.065 g g^{-1}) (Table 7). Comparison of these values with those recorded when the regression equations
301 were established with the data of Bruand and Tessier (2000) showed that the range of bias for water
302 potential ranging from -10 to -15000 hPa was reduced by 20%, with no variation in the precision
303 when the regression equations were established with both the datasets (Table 7). The overall
304 prediction quality was slightly increased, as indicated by the *RMSE* values which were reduced by
305 20% when the regression equations were established using both datasets (Table 7).

306 Thus, when clayey soils with clays developing a high CEC and a hydric history acquired in a
307 semi-arid climate are taken into account, this slightly improves the validity of using $V_{p,cl}$ to predict the
308 water retention properties of the clay of horizons belonging to soils developed under a larger range of
309 climatic environments than those already studied in the literature.

310

311 ***Water retention curve of the horizons***

312 The regression equations established between W_{cl} and $V_{p,cl}$ make it possible to predict the water
313 content at the scale of the horizon since:

314
$$W_i = CC \times [a_i + (b_i \times V_{p,cl})] \quad (13)$$

315 with W_i , the gravimetric water content in g of water per g of oven-dried soil at the water potential i ,
 316 CC , the clay content of the soil in g of clay per g of oven-dried soil, a_i and b_i , the coefficients of the
 317 regression equations at the water potential i (Table 6), and $V_{p,cl}$, the specific pore volume of the clay in
 318 cm^3 per g of oven-dried clay for the soil at field capacity. The predicted volumetric water content at
 319 water potential i (θ_i , in cm^3 of water per cm^3 of soil) can be calculated as follows:

320
$$\theta_i = D_b \times W_i. \quad (14)$$

321 Then, by using equations (7), (8) and (11):

322
$$\theta_i = D_b \times CC \times \{a_i + [b_i \times ((1/D_b) - V_s)/CC]\} \quad (15)$$

323 which becomes:

324
$$\theta_i = D_b \times CC \times \{a_i + [b_i \times ((1/D_b) - 0.377)/CC]\} \quad (16)$$

325 using $V_s = 0.377 \text{ cm}^3 \text{ g}^{-1}$ which corresponds to a particle density of 2.65. The θ_i calculated at the
 326 different water potentials and for the different horizons were compared to the θ_i measured. Results
 327 showed ME ranging from $-0.028 \text{ cm}^3 \text{ cm}^{-3}$ at -33 hPa water potential to $0.025 \text{ cm}^3 \text{ cm}^{-3}$ at -1000 hPa
 328 water potential (mean = $-0.005 \text{ cm}^3 \text{ cm}^{-3}$), SD from $0.036 \text{ cm}^3 \text{ cm}^{-3}$ at -15000 hPa water potential to
 329 $0.054 \text{ cm}^3 \text{ cm}^{-3}$ at -10 and -33 hPa water potential (mean = $0.046 \text{ cm}^3 \text{ cm}^{-3}$) and $RMSE$ from 0.039
 330 $\text{cm}^3 \text{ cm}^{-3}$ at -3300 hPa water potential to $0.059 \text{ cm}^3 \text{ cm}^{-3}$ at -33 hPa water potential (mean = 0.048
 331 $\text{cm}^3 \text{ cm}^{-3}$) (Table 8).

332 These results can be compared with those recorded earlier with soils located in semi-arid areas.
 333 Tombul et al. (2004) applied early pedotransfer functions established using multiple linear regression
 334 to 126 horizons originating from soils developed in a semi-arid area in Turkey. They compared the
 335 measured and predicted volumetric water contents at -330 and -15000 hPa and recorded a mean
 336 $RMSE$ of 0.072 and $0.030 \text{ cm}^3 \text{ cm}^{-3}$, respectively. Mosaddeghi and Mahboubi (2011) studied the water

337 retention properties of 63 soils located in a semi-arid area of western Iran. They developed
338 pedotransfer functions using multiple linear regression and the comparison of the measured and
339 predicted volumetric water content at 11 water potentials between -10 and -15000 hPa led to *RMSE*
340 ranging from 0.034 to 0.044 $\text{cm}^3 \text{cm}^{-3}$ for the 63 topsoils and from 0.034 to 0.047 $\text{cm}^3 \text{cm}^{-3}$ for the
341 subsoils. More recently, Dharumarajan et al. (2019) established pedotransfer functions using also
342 multiple linear regression for soils developed in a semi-arid area of India. They studied 740 horizons
343 originating from 149 soils with varying textures. The *RMSE* recorded when they compared the
344 measured and predicted volumetric water content at -330 and -15000 hPa was 0.046 and 0.032
345 $\text{cm}^3 \text{cm}^{-3}$, respectively.

346 Using multiple linear regression, artificial neural networks and support vector machines, Khlosi et
347 al. (2016) discussed the performance of pedotransfer functions established with Syrian soils which
348 were mainly loam, clay loam and clay soils. They applied their pedotransfer functions to 18 horizons
349 originating from Syrian soils and recorded values of *RMSE* higher than those recorded in this study
350 with *RMSE* ranging from 0.065 to 0.089 $\text{cm}^3 \text{cm}^{-3}$ (mean = 0.080 $\text{cm}^3 \text{cm}^{-3}$) with multiple linear
351 regressions, from 0.055 to 0.075 $\text{cm}^3 \text{cm}^{-3}$ (mean = 0.067 $\text{cm}^3 \text{cm}^{-3}$) with artificial neural networks and
352 from 0.048 to 0.064 $\text{cm}^3 \text{cm}^{-3}$ (mean = 0.058 $\text{cm}^3 \text{cm}^{-3}$) with support vector machines.

353 As the size of the datasets used in these different studies was highly variable and larger than in our
354 study, the comparison with our results and between the different studies remains limited to the
355 observation that the *RMSE* values are of the same order of magnitude. In our study, we used only two
356 soil characteristics, the clay content and the bulk density when the soil was close to field capacity,
357 when the above studies have used much more soil characteristics. Our results indicate for soils of
358 semi-arid areas the interest of developing pedotransfer functions which take variables closely related
359 to the water retention mechanisms in soils more into account. The values of θ calculated with the
360 proposed equations at the different water potentials can be used to fit a model of water retention curve
361 which is usually required to predict plant-available water and more generally, to run plant-soil-water
362 models. Future work will aim at enlarging both the range of textures and of climatic conditions under

363 which the clayey soils developed, with the aim of studying the way in which their water retention
364 properties are related to the hydric history.

365

366 **Conclusion**

367 Our objective was to analyze the water retention properties of clayey soils developed in semi-arid
368 areas of Syria and to discuss how these properties could be explained by the characteristics of the clay.
369 Results showed that the clay of the soils studied has both a higher cation exchange capacity and a
370 higher external specific surface area than those recorded for clayey soils studied in temperate areas and
371 used as a reference in this study. The cation exchange capacity and external specific surface area
372 values recorded are consistent with the clay mineralogy, as shown by the X-ray diffraction data which
373 revealed the presence in most horizons of a high proportion of smectite and secondarily a varying
374 proportion of illite and chlorite, while kaolinite was present but not abundant. Results also showed that
375 the amount of water retained by the clay at water potentials ranging from -10 to -15000 hPa was
376 closely related to the specific pore volume developed by the elementary clay particles at field capacity.
377 Thus, regression equations established by using both the data earlier published and those recorded in
378 this study were proposed to predict the water retention properties of clayey soils over a larger range of
379 clay mineralogies and climatic environments than previously reported in the literature. The specific
380 pore volume as well as the clay content were found to be the most important predictors of water
381 retention properties, the former corresponding to the pore volume developed by the elementary clay
382 particles which varies according to the clay mineralogy and hydric history of the soil. Finally, from a
383 more applied point of view, our results showed the significance of the bulk density measured in
384 conditions close to the field capacity to predict the water retention properties of clayey soils. It should
385 be more systematically measured during soil studies.

386

387

388 **Funding**

389 This work was funded by the Labex Voltaire (ANR-10-LABEX-100-01) and the French program
390 PAUSE.

391

392

393 **References**

394 Al Majou, H., A. Bruand A., and O. Duval. 2008a. The use of in situ volumetric water content at field
395 capacity to improve the prediction of soil water retention properties. *Canadian Journal of Soil*
396 *Science* 88(4):533–541. doi: 10.4141/CJSS07065.

397 Al Majou, H., A. Bruand, O. Duval, C. Le Bas, and A. Vautier. 2008b. Prediction of soil water
398 retention properties after stratification by combining texture, bulk density and the type of horizon.
399 *Soil Use and Management* 24(4):383–391. doi: 10.1111/j.1475-2743.2008.00180.x.

400 Al Majou, H., B. Hassani, and A. Bruand. 2018. Transferability of continuous- and class-pedotransfer
401 functions to predict water retention properties of semiarid Syrian soils. *Soil Use and Management*
402 34(3):354–369. doi: 10.1111/sum.12424.

403 Baize, D. 2018. Guide des analyses en pédologie. Quae, Paris.

404 Balbino, L., A. Bruand, I. Cousin, M. Brossard, P. Quétin, and M. Grimldi. 2004. Change in the
405 hydraulic properties of a Brazilian clay Ferralsol on clearing for pasture. *Geoderma* 120 (3–4):297–
406 307. doi: 10.1016/j.geoderma.2003.08.017.

407 Bergaya, F., and G. Lagaly. 2013. *Handbook of clay science*, volume 5, Elsevier, 1752p.

408 Bigorre, F., D. Tessier, and G. Pédro. 2000. Significance of CEC and surface area of soils. How clay
409 and organic matter contribute to water retention properties. *Comptes Rendus de l'Académie des*
410 *Sciences, Série II, Sciences de la Terre et des Planètes* 330(4):245–250. doi: 10.1016/S1251-
411 8050(00)00136-1.

412 Boivin, P., Garnier, P., and D. Tessier. 2004. Relationship between clay content, clay type, and
413 shrinkage properties of soil samples. *Soil Science of America Journal* 68(4):1145-1153.

414 Bouma, J., and J.A.J. Van Lanen. 1987. Transfer functions and threshold values: From soil
415 characteristics to land qualities. In: K.J. Beek et al. (Eds), *Quantified Land Evaluation*. Proceedings
416 of the ISS and SSSA Workshop, Washington, DC. 27 Apr. – 2 May 1986. International Institute for
417 Aerospace Survey Earth Sciences Publ. No. 6 ITC Publ., Enschede, the Netherlands, pp 106–110.

418 Bruand, A., O. Duval, H. Gaillard, R. Darthout, and M. Jamagne. 1996. Variabilité des propriétés de
419 rétention en eau des sols: importance de la densité apparente. *Etude et Gestion des Sols* 3 :27–40.

420 Bruand, A., and R. Prost. 1986. Apport des méthodes d'enrichissement sélectives et des spectrométries
421 à l'identification des constituants minéraux d'un échantillon de sol. *Agronomie* 6(8):717–726. doi:
422 10.1051/agro :19860804.

423 Bruand, A., and D. Zimmer. 1992. Relation entre la capacité d'échange cationique et le volume poral
424 dans les sols argileux : incidence sur la morphologie de la phase argileuse à l'échelle des
425 assemblages élémentaires. *Comptes Rendus de l'Académie des Sciences* 315, série II:223–229.

426 Bruand, A. and D. Tessier. 2000. Water retention properties of the clay in soils developed on clayey
427 sediments: Significance of parent material and soil history. *European Journal of Soil Science*
428 51:679–688. doi: 10.1111/j.1365-2389.2000.00338.x

429 Churchman, G.J., and B. Velde. 2019. *Soil clays. Linking geology, biology, agriculture, and the*
430 *environment*. CRC Press, Taylor & Francis Group: 294p. doi: //doi.org/10.1201/9780429154768

431 D'Angelo, B., A. Bruand, J. Qin, X. Peng, C. Hartmann, B. Sun, H. Hao, O. Rozenbaum, and F.
432 Muller. 2014. Origin of the high sensitivity of Chinese red clay soils to drought: significance of the
433 clay characteristics. *Geoderma* 223–225:46–53. doi: 10.1016/j.geoderma2014.01.09

434 De Paepe, J.L., A.A. Bono, and R. Alvarez. 2018. Simple estimation of available water capacity in
435 soils of semiarid and subhumid environments. *Arid Land Research and Management* 32(2):133–
436 148. doi: 10.1080/15324982.2017.1408153.

437 Dharumarajan, S., R. Hegde, M. Lalitha, B. Kalaiselvi, and K. Singh. 2019. Pedotransfer functions for
438 predicting soil hydraulic properties in semi-arid regions of Karnataka Plateau, India. *Current*
439 *Science* 116(7):1237–1246. doi: 10.18520/cs/v116/i7/1237-1246.

440 Dupuis M. 1969. Dosage des carbonates dans les fractions granulométriques de quelques sols calcaires
441 et dolomitiques. *Annales Agronomiques* 20:61–88.

442 Ethan, S., and A. Umar. 2001. Water conservation and management in semi-arid and arid lands for
443 sustainable agriculture. *Journal of Sustainable Agriculture* 18(1):99–108. doi:
444 10.1300/J064v18n01_08.

445 Fripiat, J., J. Chaussidon, and A. Jelli. 1971. *Chimie-Physique des phénomènes de surface. Application*
446 *aux oxydes et aux silicates*. Masson Paris. 387p.

447 Gaiser, T., F. Graef, and J.C. Cordiero. 2000. Water retention characteristics of soils with contrasting
448 clay mineral composition in semi-arid tropical regions. *Australian Journal of Soil Research*
449 38(3):523–536. doi: 10.1071/SR99001.

450 ISSS Working Group WRB. 2015. World Reference Base for Soil Resources 2014, update
451 2015. International soil classification system for naming soils and creating legends for soil
452 maps. World Soil Resources Reports No 106. FAO, Roma.

453 Kalumba, M., B. Bamps, I. Nyambe, S. Dondeyne, and J. Van Orshoven. 2020. Development and
454 functional evaluation of pedotransfer functions for soil hydraulic properties for the Zambezi River
455 Basin. *European Journal of Soil Science*. doi: 10.1111/ejss.13077.

456 Khlosi, M., M. Alhamdoosh, A. Douaik, D. Gabriels and W.M. Cornelis. 2016. Enhanced pedotransfer
457 functions with support vector machines to predict water retention of calcareous soil. *European*
458 *Journal of Soil Science*, 67, 276-284. doi: 10.1111/ejss.12345.

459 Khlosi, M., W.M. Cornelis, and D. Gabriels. 2012. Exploration of the interaction between hydraulic
460 and physicochemical properties of Syrian soils. *Vadose Zone Journal*. doi: 10.2136/vzj2012.0209.

461 Land Classification and Soil Survey of the Syrian Arab Republic, 1982. (Reconnaissance Soil Survey
462 of Syria, 1: 500,000). Louis Berger International Inc., Remote Sensing Institute South Dakota
463 University, United States Agency for International Development, *Washington DC*, 2.

464 Mason, S., C. Stephen, K. Ouattara, S.J.B. Taonda, S. Pale, A. Sohero, and D. Kabore. 2015. Soil and
465 cropping system research in semi-arid West Africa as related to the potential for conservation
466 agriculture. *Journal of Agricultural Sustainability* 13(2):120–134. doi:
467 10.1080/14735903.2014.945319.

468 Monnier, G., P. Stengel, and J.C. Fiès 1973. Une méthode de mesure de la densité apparente de petits
469 agrégats terreux. Application à l'analyse des systèmes de porosité du sol. *Annales Agronomiques*
470 24:533–545.

471 Moore, D.M., and R.C. Reynolds. 1997. X-ray diffraction and the identification and analysis of clay
472 minerals, 2nd ed., Oxford, New York, Oxford University Press.

473 Moret-Fernandez, D., C. Castaneda, Y. Puevo, C.G. Bueno, and J. Herrero. 2013. Hydro-Physical
474 Behavior of Gypseous Soils Under Different Soil Management in a Semiarid Region of NE Spain.
475 *Arid Land Research and Management* 27(1):1–16. doi: 10.1080/15324982.2012.719573.

476 Mosaddeghi, M.R., and A.A. Mahboubi. 2011. Point pedotransfer functions for prediction of water
477 retention of selected soil series in a semi-arid region of western Iran. *Archives of Agronomy and*
478 *Soil Science* 57(4): 327–342. doi: 10.1080/03650340903386313.

479 Mrabet, R. 2011. Climate change and carbon sequestration in the Mediterranean basin: contributions
480 of no-tillage systems. 4^{ème} Rencontres Méditerranéennes du Semis Direct. *Options*
481 *Méditerranéennes*, 96:165–184.

482 Ostovari, Y., K. Asgari, and W. Cornelis. 2015. Performance Evaluation of Pedotransfer Functions to
483 Predict Field Capacity and Permanent Wilting Point Using UNSODA and HYPRES Datasets. *Arid*
484 *Land Research and Management* 29(4):383–398. doi: 10.1080/15324982.2015.1029649.

485 Quirk J.P., 1994. Interparticle forces: a basis for the interpretation of soil physical behaviour,
486 *Advances in Agronomy* 53: 121–183.

487 Reatto, A., A. Bruand, E.M. Silva, E.S. Martins, and M. Brossard. 2007. Hydraulic properties of the
488 diagnostic horizon of Latosols of a regional toposequence across the Brazilian Central Plateau.
489 *Geoderma* 139(1-2): 51 – 59. doi: 10.1016/j.geoderma.2007.01.003.

490 Rigot, J.B. 2006. L'évolution ralentie du milieu naturel dans la steppe aride du Nord de la Syrie à
491 l'Holocène. *Géomorphologie : Relief, Processus, Environnement* 4 :259–274.

492 Robert, M., and Tessier. 1974. Méthode de préparation des argiles des sols pour les études
493 minéralogiques. *Annales Agronomiques* 25:859–882.

494 Robert, M., M. Hardy. and F. Elsass. 1991. Crystallochemistry, properties and organization of soil
495 clays derived from major sedimentary rocks in France. *Clay Minerals* 26:409–420.

496 Santra, P., M. Kumar, R.N. Kumawat, D.K. Painuli, K.M. Hati, Heuvelink G.B.M., and N.H. Batjes.
497 2018. Pedotransfer functions to estimate soil water content at field capacity and permanent wilting
498 point in hot Arid Western India. *Journal of Earth System Science* 127(3):35. doi: 10.1007/s12040-
499 018-0937-0.

500 Schellekens, J., G.G. Barberá., P. Buurman, G. Pérez-Jordà, and A. Martínez-Cortizas. 2013. Soil
501 organic matter dynamics in Mediterranean A-horizons e the use of analytical pyrolysis to ascertain
502 land use history. *Journal of Analytical and Applied Pyrolysis* 104:287–298. doi:
503 10.1016/j.jaap.2013.07.004.

504 Schnitzer, M. 1978. Humic substances: chemistry and reactions. In: Schnitzer M. and Khan S.U.(eds)
505 Soil organic matter, Elsevier, New York, pp 1–58.

506 Singh, A., A. Haghverdi, H.S. Ozturk, and W. Durner. 2020. Developing Pseudo Continuous
507 Pedotransfer Functions for International Soils Measured with the Evaporation Method and the
508 HYPROP System: I. The Soil Water Retention Curve. *Water* 12(12):3425. doi:
509 10.3390/w12123425.

510 Soil Survey Staff. 2010. Keys to Soil Taxonomy. Washington, DC: United States Department of
511 Agriculture. Natural Resources Conservation Service.

512 Soleimani, R., E. Chavoschi, H. Shirani, and I.E. Pour. 2020. Comparison of Stepwise Multilinear
513 Regressions, Artificial Neural Network, and Genetic Algorithm-Based Neural Network for
514 Prediction the Plant Available Water of Unsaturated Soils in a Semi-arid Region of Iran (Case
515 Study: Chaharmahal Bakhtiari Province). *Communications in Soil Sciences and Plant Analysis*
516 51(17): 2297–2309. doi: 10.1080/00103624.2020.1822385

517 Stevenson F.J. 1982. Humus chemistry: genesis, composition, reactions. John Wiley, New York, 443
518 pp.

519 Tate K.R. and B.K.G Theng. 1980. Organic matter and its interactions with inorganic constituents (ed.
520 B.K.G. Theng) Soils with variable charges, New Zealand Society of Soil Science, Lower Hutt, pp.
521 225-249.

522 Tawornpruek, S., I. Kheoruenromme, A. Suddhiprakarn, and R.J. Gilkes. 2005. Microstructure and
523 water retention of Oxisols in Thailand. *Australian Journal of Soil Research* 43(8): 973–986. doi:
524 10.1071/SR05039.

525 Tessier D., and G. Pédro. 1984. Recherches sur le rôle des minéraux argileux dans l'organisation et le
526 comportement des sols. Association Française pour l'Étude des Sols, Livre Jubilaire: 223–234.

527 Tessier D., and G. Pédro. 1987. Mineralogical characterization of 2:1 clays in soils: importance of the
528 clay texture. In: Proceedings of the International Clay Conference. Denver, 1985 (eds L.G. Schultz,
529 H. van Olphen and F.A. Mumpton), pp. 78–84. The Clay Minerals Society, Bloomington, IN.

530 Tessier, D., A. Lajudie, and J.C. Petit. 1992. Relation between the macroscopic behavior of clays and
531 their microstructural properties. *Applied Geochemistry* 7(1):151–161.

532 Tombul, M., Z. Akyürek, and A.Ü. Sorman. 2004. Determination of soil hydraulic properties using
533 pedotransfer functions in a semi-arid basin. *Hydrology and Earth System Sciences* 8(6):1200–1209.
534 doi: 10.5194/hess-8-1200-2004

535 Tóth, B., A. Makó, A. Guadagini, and G. Tóth. 2012. Water retention of salt-affected soils:
536 quantitative estimation using soil survey information. *Arid Land Research and Management*
537 26(2):103–121. doi: 10.1080/15324982.2012.657025.

538 Wilson M.J. 1999. The origin and formation of clay minerals in soils: past, present and future
539 perspectives. *Clay Minerals* 34(1):7–25. doi: 10.1180/000985599545957.

540 Wösten, J.H.M. Lilly, A. Nemes, A., and C. Le Bas. 1999. Development and use of a database of
541 hydraulic properties of European soils. *Geoderma* 90(3–4): 169–185. doi: 10.1016/S0016-
542 7061(98)00132-3.

543 Xu Xu, H.W. Li, C. Su, T.B. Ramos, H. Darouich, Y.W. Xiong, Z.Y. Xiong, and G.H. Huang. 2021.
544 Pedotransfer functions for estimating soil water retention properties of northern China agricultural
545 soils: Development and needs. *Irrigation and Drainage In Press*. doi: 10.1002/ird.2584.
546

547 **List of Figures**

548

549 **Figure 1.** X-ray diagrams of oriented deposits of the clay material extracted from the clayey horizons
550 studied under room conditions (20 °C), after saturation with ethylene-glycol (EG), after heating at 150
551 °C and 550 °C.

552

553 **Figure 2.** Relation between the cation exchange capacity of the clay (CEC_{cl}) and the specific surface
554 area of the clay (SSA_{cl}) for both the clayey soils studied by Bruand and Tessier (2000) (o) and the
555 Syrian clayey soils of this study (●).

556

557

558 **List of tables**

559

560 **Table 1.** Main characteristics of the soils studied.

561

562 **Table 2.** Main characteristics of the horizons studied.

563

564 **Table 3.** Semi-quantitative evaluation of clay minerals identified by DRX.

565

566 **Table 4.** Water content at field conditions (W_{fc} , g g⁻¹) and at different water potentials (W_h , g g⁻¹).

567

568 **Table 5.** Characteristics calculated for the clay of the Syrian soils studied.

569

570 **Table 6.** Regression equations between the water content of clay (W_{cl}) at different water potentials and
571 the clay fabric ($V_{p, cl}$) calculated with the data published in tables 1, 2 and 3 by Bruand and Tessier
572 (2000).

573

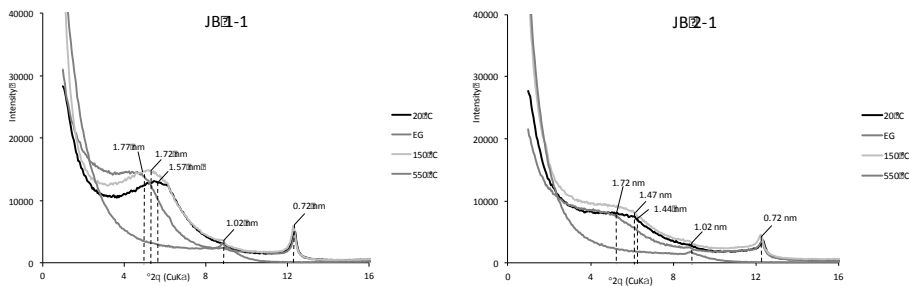
574 **Table 7.** Mean error of prediction (ME), standard deviation (SD) and root mean square error ($RMSE$)
575 recorded with the regression equations established between the gravimetric water content of clay (W_{cl} ,
576 in g g⁻¹ of oven dried clay) at different water potentials and the pore volume developed by the
577 elementary clay particles ($V_{p, cl}$, in cm³ g⁻¹ of oven dried clay) at field capacity.

578

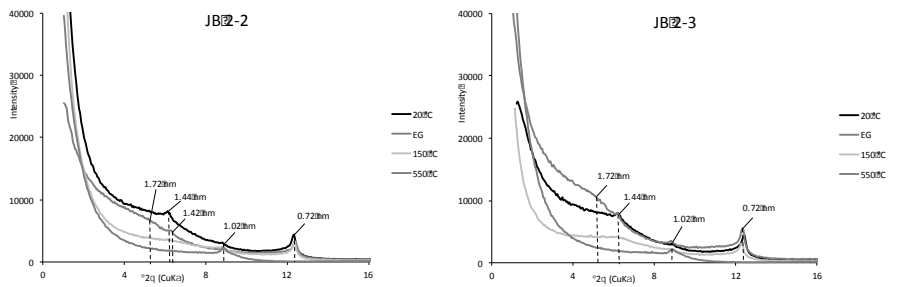
579 **Table 8.** Mean error of prediction (ME), standard deviation (SD) and root mean square error ($RMSE$)
580 recorded with the regression equations established between the volumetric water content of clay (θ_h , in
581 cm³ cm⁻³) at different water potentials h and both the clay content and the reciprocal of bulk density
582 measured in conditions close to field capacity with both the data published by Bruand and Tessier
583 (2000) and those recorded in this study when applied to the horizons of this study.

584

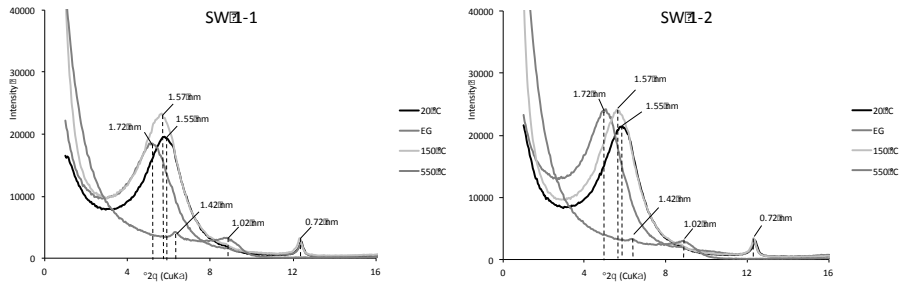
585



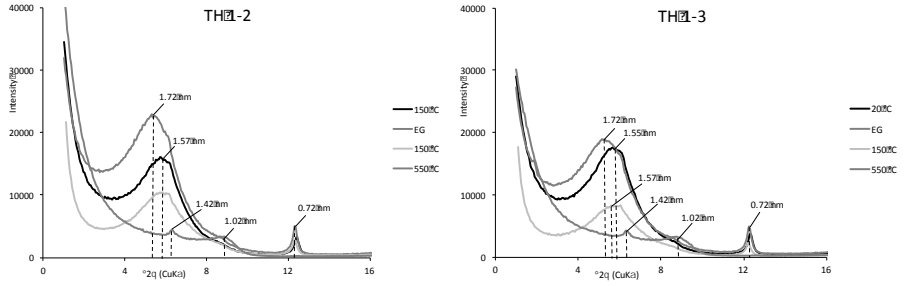
586



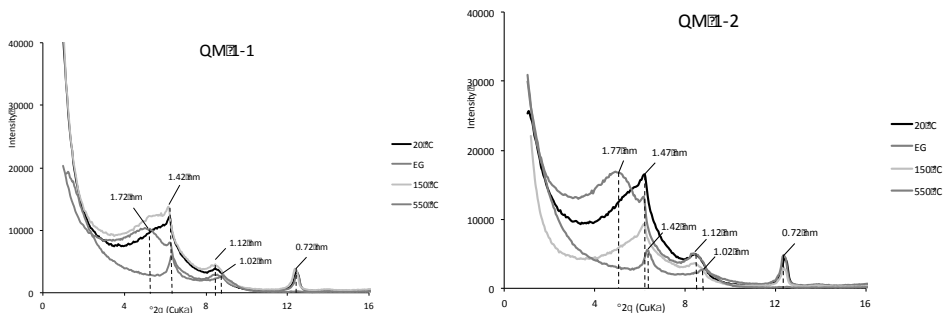
587



588



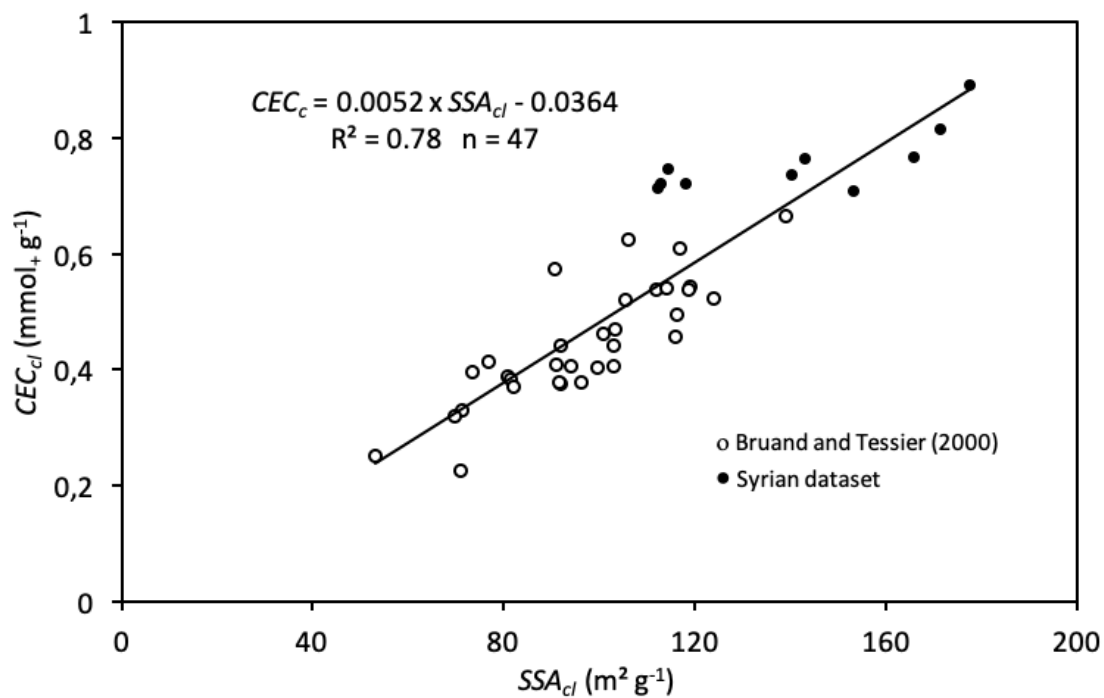
589



590

591 **Figure 1.** X-ray diagrams of oriented deposits of the clay material extracted from the clayey horizons
592 studied under room conditions (20 °C), after saturation with ethylene-glycol (EG), after heating at 150
593 °C and 550 °C.

594



596

597 **Figure 2.** Relation between the cation exchange capacity of the clay (CEC_{cl}) and the specific surface
598 area of the clay (SSA_{cl}) for both the clayey soils studied by Bruand and Tessier (2000) (o) and the
599 Syrian clayey soils of this study (●).

600

601

602

603

604 **Table 1.** Main characteristics of the soils studied.

Soil location	Coordinates UTM	Soil type Soil Survey Staff (2010) / IUSS Working Group WRB (2015)	Parent material	Land use	Agro-climatic zone
Jabbah (JB 1)	33.1623N – 35.9368E	Typic Haploxerept / Hypereutric Cambisol		Meadow	1
Jabbah (JB 2)	33.1520N – 35.9243E	Typic Haploxerept / Hypereutric Cambisol	Clayey surface formations	Meadow	1
Al-Suwayda (SW 1)	32.7118N – 36.5494E	Vertic Chromoxerept / Chromic Vertisol	including coarse elements of basic extrusive rocks	Annual crops	2
Al-Tha'Ala (TH 1)	32.7115N – 36.4860E	Vertic Xerochept / Chromic Vertisol		Olive trees	2
Al-Qamishli (QM 1)	41.0324N – 41.1303E	Calcic Xerocept / Vertic Calcisol	Calcareous alluvium materials	Annual crops	1

605 Agro-climatic zones according to Khlosi et al. (2012): zone 1 is characterized by a mean annual precipitation >300 mm in 2 out of 3 seasons and shrubland, degraded forest, rock outcrops and
606 permanent crops; zone 2 is characterized by a mean annual precipitation of 250-300 mm 2 out of 3 seasons, permanent crops and rainfed field crops with irrigated crops.

607

608

609

610

611 **Table 2.** Main characteristics of the horizons studied.

Soil Sample	Horizon	Depth cm	Texture	D_b	Particle size distribution			CaCO_3 $\text{g}\cdot\text{g}^{-1}$	OC $\text{g}\cdot\text{g}^{-1}$	CEC $\text{mmol}_+\cdot\text{g}^{-1}$	Exchangeable cations				SSA $\text{m}^2\cdot\text{g}^{-1}$
					$\text{g}\cdot\text{g}^{-1}$						$\text{mmol}_+\cdot\text{g}^{-1}$				
					Clay <2 μm	Silt 2- 50 μm	Sand 50- 2000 μm				Ca ²⁺	Mg ²⁺	Na ⁺	K ⁺	
JB 1-1	A	5-25	F	1.48	0.43	0.34	0.23	≤0.01	0.008	0.304	0.180	0.086	0.019	0.010	65.9
JB 2-1	A	5-25	F	1.49	0.45	0.29	0.26	≤0.01	0.008	0.345	0.202	0.099	0.020	0.010	74.7
JB 2-2	B	30-60	F	1.44	0.46	0.30	0.24	≤0.01	0.004	0.375	0.208	0.113	0.016	0.008	78.9
JB 2-3	B	60-80	F	1.41	0.46	0.31	0.23	0.02	0.002	0.410	0.209	0.116	0.010	0.007	81.7
SW 1-1	A	0-25	F	1.26	0.58	0.22	0.20	0.04	0.004	0.442	0.306	0.097	0.008	0.009	83.0
SW 1-2	B	30-70	VF	1.28	0.65	0.16	0.19	0.05	0.002	0.478	0.333	0.093	0.010	0.007	91.3
TH 1-2	B	25-50	VF	1.28	0.66	0.15	0.19	0.06	0.003	0.475	0.294	0.119	0.016	0.011	74.6
TH 1-3	B	50-75	VF	1.25	0.69	0.11	0.20	0.06	0.002	0.492	0.317	0.082	0.024	0.008	77.6
QM 1-1	A	0-25	F	1.32	0.53	0.25	0.22	0.30	0.006	0.395	0.290	0.082	0.010	0.005	60.8
QM 1-2	B	25-50	F	1.34	0.57	0.24	0.19	0.31	0.004	0.410	0.320	0.089	0.006	0.003	67.4
Mean	–	–	–	1.36	0.55	0.24	0.21	0.087	0.004	0.413	0.266	0.098	0.014	0.008	75.6
SD	–	–	–	0.09	0.09	0.08	0.03	0.111	0.002	0.058	0.059	0.014	0.006	0.002	8.6
Min	–	–	–	1.25	0.43	0.11	0.19	0.01	0.002	0.305	0.180	0.082	0.006	0.003	60.8
Max	–	–	–	1.49	0.69	0.34	0.26	0.31	0.008	0.492	0.333	0.119	0.024	0.011	91.3

612 Texture according to the FAO triangle (FAO, 1990), F: Fine, VF: Very Fine; D_b , bulk density; CaCO_3 , calcium carbonate content; OC : organic carbon content; CEC , cation exchange capacity; SD ,
613 standard deviation.
614

615
616
617

Table 3. Semi-quantitative evaluation of clay minerals identified by DRX.

Soil Sample	Clay minerals			
	Kaolinite	Illite	Smectite	Chlorite
JB 1-1	+	+	++	-
JB 2-1	+	+	+	-
JB 2-2	+	+	+	-
JB 2-3	+	+	+	-
SW 1-1	+	-	+++	+
SW 1-2	+	-	+++	+
TH 1-2	+	-	+++	+
TH 1-3	+	-	+++	+
QM 1-1	+	++	++	++
QM 1-2	+	++	++	++

618 +++ abundant, ++ moderately abundant, + not abundant, - not identified.

619
620
621

622 **Table 4.** Water content at field conditions (W_{fc} , g g^{-1}) and at different water potentials (W_h , g g^{-1}).

Soil sample	W_{fc}	Water retained at a water potential of hPa (g g^{-1})						
		W_{-10}	W_{-33}	W_{-100}	W_{-330}	W_{-1000}	W_{-3300}	W_{-15000}
JB 1-1	0.318	0.360	0.343	0.303	0.272	0.261	0.242	0.222
JB 2-1	0.262	0.331	0.301	0.284	0.254	0.241	0.236	0.207
JB 2-2	0.283	0.328	0.320	0.296	0.261	0.248	0.244	0.224
JB 2-3	0.292	0.342	0.330	0.317	0.265	0.251	0.245	0.224
SW 1-1	0.371	0.445	0.439	0.433	0.352	0.320	0.316	0.279
SW 1-2	0.375	0.447	0.424	0.408	0.340	0.338	0.322	0.279
TH 1-2	0.472	0.534	0.508	0.468	0.431	0.311	0.302	0.270
TH 1-3	0.507	0.540	0.532	0.483	0.451	0.423	0.414	0.385
QM 1-1	0.342	0.402	0.397	0.342	0.299	0.287	0.265	0.249
QM 1-2	0.344	0.382	0.357	0.341	0.302	0.290	0.264	0.255
Mean	0.357	0.411	0.395	0.368	0.323	0.297	0.285	0.259
SD	0.075	0.075	0.076	0.070	0.067	0.052	0.053	0.048
Min	0.262	0.328	0.301	0.284	0.254	0.241	0.236	0.207
Max	0.507	0.540	0.532	0.483	0.451	0.423	0.414	0.385

SD, standard deviation.

623
624
625
626

627
628
629

Table 5. Characteristics calculated for the clay of the Syrian soils studied.

Soil Sample	CEC_{cl} $\text{mmol}_+, \text{g}^{-1}$	SSA_{cl} $\text{m}^2 \cdot \text{g}^{-1}$	$V_{p, cl}$ $\text{cm}^3 \cdot \text{g}^{-1}$
JB 1-1	0.707	153	0.695
JB 2-1	0.767	166	0.654
JB 2-2	0.815	172	0.690
JB 2-3	0.891	178	0.722
SW 1-1	0.762	143	0.718
SW 1-2	0.735	141	0.622
TH 1-2	0.720	113	0.613
TH 1-3	0.712	112	0.612
QM 1-1	0.745	115	0.718
QM 1-2	0.719	118	0.648
Mean	0.757	141	0.669
SD	0.054	24	0.042
Min	0.707	112	0.612
Max	0.891	178	0.722

630 CEC_{cl} , cation exchange capacity of the clay; SSA_{cl} , specific surface
631 area of the clay; $V_{p, cl}$, specific pore volume of the clay
632

633
634
635
636

637
638
639
640

Table 6. Regression equations between the water content of clay (W_{cl}) at different water potentials and the clay fabric ($V_{p,cl}$) calculated with the data published in tables 1, 2 and 3 by Bruand and Tessier (2000).

Water potential hPa	Regression equations calculated:					
	with the data published by Bruand and Tessier (2000) (n=37)			with both the data published by Bruand and Tessier (2000) and those recorded in this study (n=10)		
		R ²	N		R ²	N
-10	$W_{cl} = -0.0184 + 1.0516 V_{p,cl}$	0.96	37	$W_{cl} = -0.0107 + 1.0615 V_{p,cl}$	0.92	47
-33	$W_{cl} = -0.0150 + 1.0327 V_{p,cl}$	0.96	37	$W_{cl} = -0.0087 + 1.0378 V_{p,cl}$	0.93	47
-100	$W_{cl} = -0.0310 + 1.026 V_{p,cl}$	0.96	37	$W_{cl} = -0.0244 + 1.0201 V_{p,cl}$	0.94	47
-330	$W_{cl} = -0.0231 + 0.9779 V_{p,cl}$	0.96	37	$W_{cl} = -0.0135 + 0.9474 V_{p,cl}$	0.92	47
-1000	$W_{cl} = -0.0027 + 0.8865 V_{p,cl}$	0.96	37	$W_{cl} = +0.0030 + 0.8613 V_{p,cl}$	0.92	47
-3300	$W_{cl} = +0.0484 + 0.7387 V_{p,cl}$	0.95	37	$W_{cl} = +0.0531 + 0.7239 V_{p,cl}$	0.91	47
-15000	$W_{cl} = +0.1462 + 0.4269 V_{p,cl}$	0.84	37	$W_{cl} = +0.1479 + 0.4388 V_{p,cl}$	0.77	47

641
642
643
644
645
646
647

648
649
650 **Table 7.** Mean error of prediction (*ME*), standard deviation (*SD*) and root mean square error (*RMSE*)
651 recorded with the regression equations established between the gravimetric water content of clay (W_{cl} , in
652 $g\ g^{-1}$ of oven dried clay) at different water potentials and the pore volume developed by the elementary
653 clay particles ($V_{p,cl}$, in $cm^3\ g^{-1}$ of oven dried clay) at field capacity.

Water potential hPa	<i>ME, SD and RSME</i> recorded with the regression equations established:								
	with the data published by Bruand and Tessier (2000) when applied to: (n=37)			with both the data published by Bruand and Tessier (2000) and those recorded in this study when applied to: (n=46)					
	the horizons of this study (n=10)			the horizons studied by Bruand and Tessier (2000) (n=37)			the horizons of this study (n=10)		
	<i>ME</i>	<i>SD</i>	<i>RMSE</i>	<i>ME</i>	<i>SD</i>	<i>RMSE</i>	<i>ME</i>	<i>SD</i>	<i>RMSE</i>
-10	-0.065	0.067	0.091	+0.014	0.043	0.045	-0.052	0.068	0.083
-33	-0.044	0.066	0.077	+0.010	0.040	0.040	-0.035	0.067	0.073
-100	-0.014	0.058	0.056	+0.002	0.040	0.039	-0.011	0.059	0.057
-330	+0.044	0.069	0.079	-0.011	0.041	0.042	+0.034	0.070	0.075
-1000	+0.047	0.050	0.067	-0.011	0.037	0.038	+0.037	0.051	0.061
-3300	+0.021	0.049	0.051	-0.005	0.035	0.035	+0.017	0.050	0.050
-15000	-0.043	0.042	0.058	+0.011	0.040	0.041	-0.034	0.043	0.053
Mean	-0.008	0.057	0.068	0.001	0.039	0.040	-0.006	0.058	0.065
Min	-0.065	0.042	0.051	-0.011	0.035	0.035	-0.052	0.043	0.050
Max	+0.047	0.069	0.091	+0.014	0.043	0.045	+0.037	0.070	0.083

654
655
656
657

658
 659
 660
 661
 662
 663
 664
 665
 666

Table 8. Mean error of prediction (*ME*), standard deviation (*SD*) and root mean square error (*RMSE*) recorded with the regression equations established between the volumetric water content of clay (θ_v , in $\text{cm}^3 \text{cm}^{-3}$) at different water potentials *h* and both the clay content and the reciprocal of bulk density measured in conditions close to field capacity with both the data published by Bruand and Tessier (2000) and those recorded in this study when applied to the horizons of this study.

Water potential (hPa)	n=10		
	<i>ME</i> (cm^3/cm^3)	<i>SD</i> (cm^3/cm^3)	<i>RMSE</i> (cm^3/cm^3)
-10	-0.024	0.054	0.054
-33	-0.028	0.054	0.059
-100	-0.011	0.046	0.045
-330	+0.021	0.053	0.054
-1000	+0.025	0.039	0.044
-3300	+0.010	0.039	0.039
-15000	-0.025	0.036	0.042
Mean	-0.005	0.046	0.048
Min	-0.028	0.036	0.039
Max	+0.025	0.054	0.059

667
 668
 669
 670
 671